

Supporting Information

Engineering a Selective Fluorescent Sensor with High Signal-to-Background Ratio for Microalbumin Detection and Imaging

Liang Su,^{‡a} Feiyu Yang,^{‡a} Wei Li,^{*a} Haiyan Li,^a Chunjiang Wang,^b Qiuhan Wang,^{*a} Lin Yuan,^{*a}

^a State Key Laboratory of Chemo/Biosensing and Chemometrics, College of Chemistry and Chemical Engineering, Hunan University, Changsha 410082, China

^b Department of Pharmacy, The Third Xiangya Hospital, Central South University, Changsha 410013, China

[‡] These authors contributed equally.

China E-mail: lyuan@hnu.edu.cn (L. Y); liwei93@hnu.edu.cn; wangqa@hnu.edu.cn

Table of Contents

1. Experimental procedures	S3-S4
2. The synthesis and characterization of compounds	S5-S7
3. Spectra and biological studies	S8-S16
4. NMR and MS spectra of synthesis compounds	S17-S25
5. References	S25

1. Experimental Procedures

Materials and instruments. Bovine serum albumin (BSA, ≥96% purity), Human serum albumin (HSA, ≥96% purity) and proteins (alkaline phosphatase (ALP), aryl sulfatase (ARS), β-Glucuronidase (GLU), acetylcholinesterase (AChE), butyrylcholinesterase (BuChE), carboxylesterase-2 (CE2), leucine aminopeptidase (LAP), alanine aminopeptidase (APN), quinone oxidoreductase isozyme (NQO1), and Lipase) were purchased from Sigma-Aldrich Co.. Diflunisal (DIF, ≥98% purity), warfarin, propofol, salicylic acid, ibuprofen, digitoxin, indomethacin, phenylbutazone, naproxen, diclofenac, mefenamic, ketorolac, piroxicam, aspirin, and acetaminophen were purchased from Bide Pharmatech Ltd., Shanghai Aladdin BioChem Technology Co., Ltd., Shanghai Yuanye Bio-Technology Co., and so on. Bromocresol Green (BCG) dye was purchased from Nanjing Jiancheng Bioengineering Institute. All chemical reagents for synthesis were obtained from commercial suppliers and were used in the whole experiment without further purification, and solvents used were purified by standard methods before use. The water used in the whole experiment was twice-distilled water. Human urine samples were obtained from male patients. ¹H NMR and ¹³C NMR spectra were recorded on a Bruker-400 spectrometer with an internal standard (TMS). Mass spectra were performed using an LCQ Advantage ion trap mass spectrometer from Thermo Finnigan. High-resolution electron spray mass spectra (HRMS) were obtained from ESI/Q-TOF Micro TM HRMS. Fluorescence spectroscopic studies were performed in an Edinburgh Instruments F-S5 fluorescence spectrometer. A PHS-3C pH meter (INESA instruments) was used to measure pH. Cell imaging was performed on Nikon A1 plus confocal microscope (Nikon, Japan). TLC analysis and column chromatography were carried out by using silica gel plates and silica gel (mesh 200-300) columns (Yantai Jiangyou Silica Gel Development Company Limited).

Molecular Docking. The 3D geometry of the molecules (FNE3 and DIF) was constructed and optimized. The X-ray crystal structure of ligand-free HSA (PDB ID: 4k2c) and BSA (PDB ID: 4f5s) were taken from the Protein Data Bank (<http://www.rcsb.org/pdb>). The R-value and the resolution of the file were 0.213 and 3.23 Å, respectively. A study on molecular docking of the protein-ligand complex was performed by AutoDock Vina 4.2 molecular docking program [1]. The molecular docking was carried out by using a grid box size of 84.35 × 84.35 × 84.35 Å with a grid resolution of 0.375 Å. The protein was considered rigid for the docking study. All allowed torsional bonds of the ligand were considered rotatable. Other parameters are set to default. 9 docking runs with 25,000,000 energy evaluations were performed. After optimization, the docking calculations result from AutoDock Vina was rendered by PyMOL.

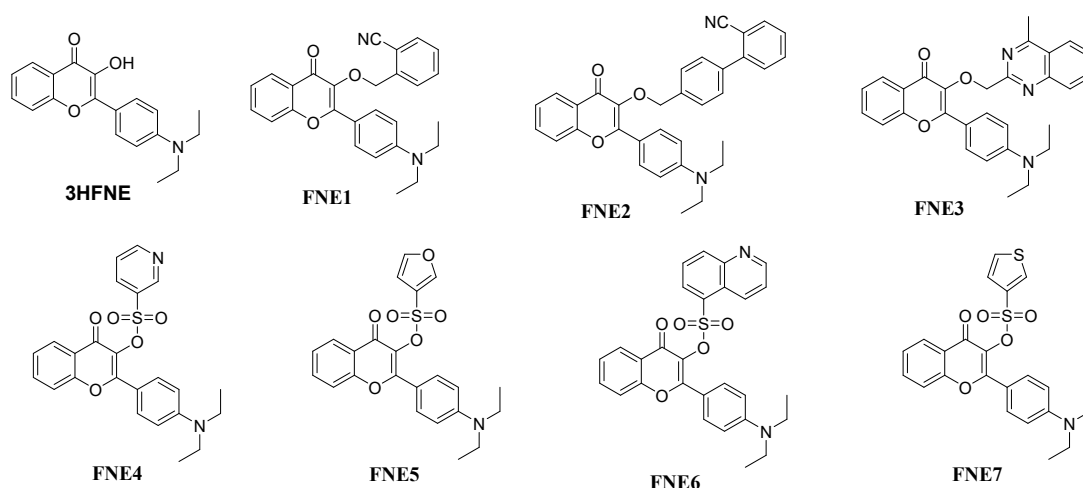
Determination of the fluorescence quantum yield. Fluorescence quantum yield for FNE3-HSA complex was determined by using coumarin 102 ($\Phi_f = 0.93$ in EtOH) as a fluorescence standard.[2] The quantum yield was calculated using the following equation:

$$\Phi_s = \Phi_r (A_r F_s / A_s F_r) (n_s^2 / n_r^2)$$

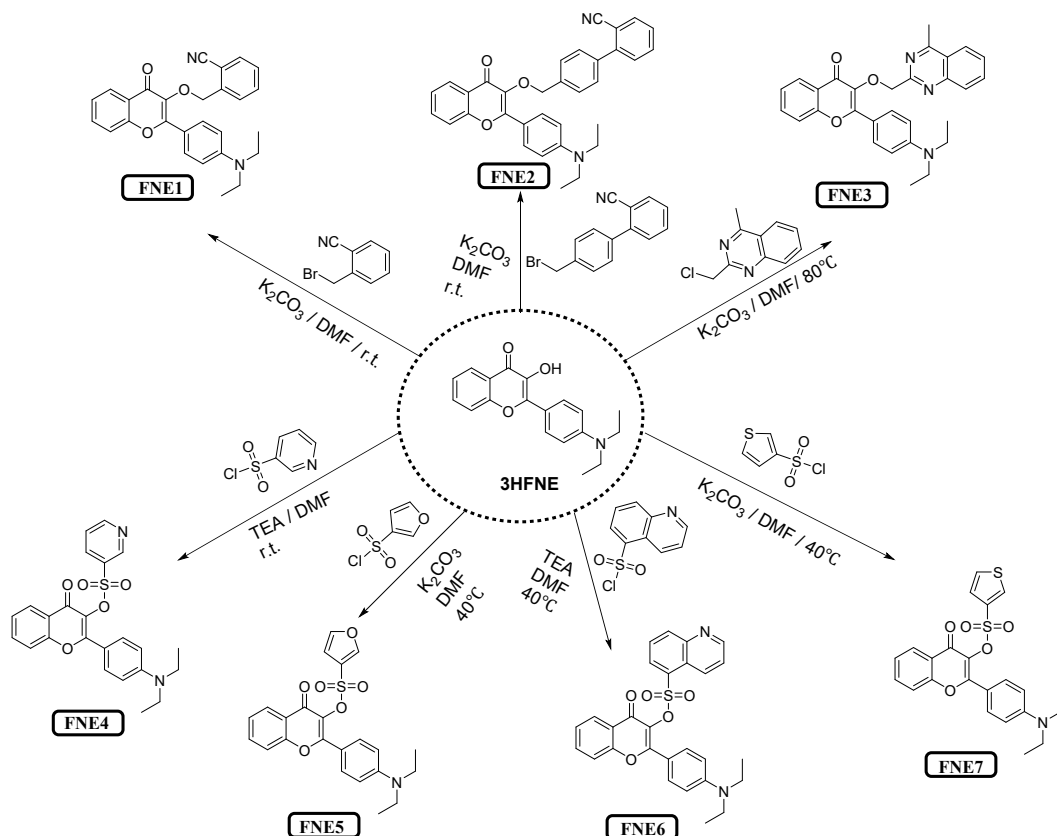
Where, s and r denote sample and reference, respectively. A is the absorbance at the excitation wavelength. F is the relative integrated fluorescence intensity and n is the refractive index of the solvent. Φ is the fluorescence quantum yield.

Cell culture and Cell cytotoxicity study. HeLa cells were cultured at 37 °C and 5% CO₂, using high glucose Dulbecco's Modified Eagle Medium (Hyclone) mixed with 10% fetal bovine serum (Gemini) and 1% antibiotics (100 U/mL penicillin and 100 µg/mL streptomycin, Hyclone). Cells were cultured in 96-well flat-bottomed plates for 24 h, and incubated FNE3 and FNE3-HSA complex. Subsequent operations were based on a standard MTT assay. Finally, the absorbance was measured at 490 nm by a multidetection microplate reader. The following formula was used to calculate the viability of cell growth: Cell viability (%) = (mean of A value of treatment group - mean of A value of control) × 100.

2. The synthesis and characterization of compounds



Scheme S1. The structure of compounds **3HFNE**, **FNE1**, **FNE2**, **FNE3**, **FNE4**, **FNE5**, **FNE6**, and **FNE7**.



Scheme S2. Synthetic routes of compounds **FNE1**, **FNE2**, **FNE3**, **FNE4**, **FNE5**, **FNE6**, and **FNE7**.

Synthesis of Compound FNE1

The compound **3HFNE** was synthesized according to literature methods.^[3] To a solution of compound **3HFNE** (10.0 g, 32.3 mmol) and 2-(bromomethyl) benzonitrile (6.34 g, 32.3 mmol) in DMF (40 mL) was added K_2CO_3 (3.4 g, 22 mmol) under rigorous stirring. The reaction mixture was stirred for 20 h at room temperature. The mixture was added water and the aqueous phase was extracted with ethyl acetate (60 mL×3). The combined organic layer was dried over

MgSO₄, which was filtered, and the filtrate was evaporated. The crude product was purified by silica gel column chromatography eluted with the mixed solution of dichloromethane and methanol (10: 1, V/V) to give compound **FNE1** as yellow solid. Yield, 9.37 g, 68.3%; m.p: 112-117°C, ¹H NMR (400 MHz, CDCl₃) δ: 8.26 (d, J = 8.0 Hz, 1H), 8.06 - 7.98 (m, 2H), 7.98 (d, J = 7.8 Hz, 1HH), 7.58-7.57 (m, 3H), 7.51 (d, J = 8.0 Hz, 1H), 7.42-7.33 (m, 2H), 6.73-6.64 (m, 2H), 5.29 (s, 2H), 3.42 (q, J = 8.0 Hz, 4H), 1.22 (m, 6H); ¹³C NMR (400 MHz, CDCl₃) δ: 174.24, 157.54, 155.08, 149.45, 140.85, 138.12, 138.59, 132.97, 132.82, 132.36, 130.33, 129.98, 128.24, 125.58, 124.44, 124.18, 117.78, 117.30, 116.35, 111.50, 110.83, 44.74, 12.58; ESI-MS: m/z calcd [C₂₇H₂₄N₂O₃] for 424.18, found [M+H]⁺ = 425.1.

Synthesis of Compound FNE2

Compound **3HFNE** (10.0 g, 32.3 mmol) and 4'-(bromomethyl)-[1,1'-diphenyl]-2-acetonitrile (8.80 g, 32.3 mmol) were added to DMF (40 mL), potassium carbonate (8.93 g, 64.6 mmol) was added under stirring, and stirred at room temperature overnight. The mixture was added water (200 mL) and the aqueous phase was extracted with ethyl acetate (60 mL × 3). The combined organic layer was dried over MgSO₄, which was filtered, and the filtrate was evaporated. The crude product was purified by silica gel column chromatography eluted with the mixed solution of dichloromethane and methanol (10/1, v/v) to give compound **FNE2** as yellow solid. Yield, 10.66 g, 65.9%; m.p: 129-132°C, ¹H NMR (400 MHz, CDCl₃) δ: 8.28 (d, J = 8.0, 1.7 Hz, 1H), 8.07 (d, J = 8.9 Hz, 2H), 7.75 (d, J = 7.7 Hz, 1H), 7.68 – 7.59 (m, 4H), 7.51 (t, J = 7.7 Hz, 4H), 7.40 (m, 2H), 6.71 (d, J = 8.0 Hz, 2H), 5.16 (s, 2H), 3.43 (m, J = 7.0 Hz, 4H), 1.21 (t, J = 7.0 Hz, 6H); ¹³C NMR (400 MHz, CDCl₃) δ: 174.49, 157.31, 155.08, 149.39, 145.26, 138.53, 137.91, 137.64, 133.74, 132.84, 130.46, 130.11, 128.98, 128.64, 127.50, 125.60, 124.32, 124.28, 118.75, 117.77, 116.72, 11.16, 110.68, 73.16, 44.44, 12.59; ESI-MS: m/z calcd [C₃₃H₂₈N₂O₃] for 500.21, found [M+H]⁺ = 501.1.

Synthesis of Compound FNE4

Compound **3HFNE** (310 mg, 1 mmol), 2-sulfonyl chloride pyridine (212 mg, 1.2 mmol), and TEA (200 mg, 2 mmol) were added to DMF (10 mL). The solution was stirred at 40 °C for 6 h. The mixture was extracted with ethyl acetate (30 mL × 3). The combined organic layer was dried over MgSO₄, which was filtered, and the filtrate was evaporated. The crude yellow oil was purified by column chromatography (ethyl acetate: petroleum ether = 1:3, V: V) to give a yellow solid. Yield, 405 mg, 90%; m.p: 143-148°C, ¹H NMR (400 MHz, CDCl₃) δ: 9.13(s, 1H, 28-H), 8.81-8.79 (m, 1H), 8.31-8.28 (m, 1H), 8.17-8.14 (m, 1H), 7.92-7.88(m, 2H), 7.69-7.64 (m, 1H), 7.52-7.49 (m, 1H), 7.43-7.36(m, 2H), 6.65 (d, J = 8.0Hz, 2H), 3.46-3.40(m, 4H), 1.22 (t, J = 8.0Hz, 6H); ¹³C NMR (100 MHz, CDCl₃) δ : 171.89, 159.63, 155.07, 153.94, 136.18, 134.64, 133.73, 131.82, 130.75, 125.97, 125.09, 123.77, 123.25, 117.81, 114.51, 110.73, 44.50, 12.59. ESI-MS: m/z calcd [C₂₄H₂₂N₂O₅S] for 450.12, found [M + H]⁺ = 451.0.

Synthesis of Compound FNE5

Compound **3HFNE** (310 mg, 1 mmol), 3-furanesulfonyl chloride (200 mg, 1.2 mmol), and TEA (200 mg, 2 mmol) were added to DMF (10 mL). The solution was stirred at 40 °C for 6 h. The mixture was extracted with ethyl acetate (30 mL × 3). The combined organic layer was dried over MgSO₄, which was filtered, and the filtrate was evaporated. The crude yellow oil was purified by column chromatography (ethyl acetate: petroleum ether = 1: 5, V: V) to give a yellow solid. Yield, 340 mg, 77 %; m.p: 136-142°C, ¹H NMR (400 MHz, CDCl₃) δ: 8.20 (dd, J = 4.0, 8.0 Hz 1H), 8.07-8.06 (m, 1H), 7.95 (d, J = 12.0 Hz, 2H), 7.64 (t, J = 8.0 Hz, 1H), 7.50 – 7.35 (m, 3H), 6.89 (d, 1H), 6.68 (d, J =

12.0 Hz, 2H), 3.41 (m, 4H), 1.20 (t, J = 8.0 Hz, 6H).¹³C NMR (100 MHz, CDCl₃) δ: 171.98, 159.60, 155.06, 150.17, 147.77, 143.93, 133.63, 131.72, 130.79, 125.91, 125.11, 124.98, 123.89, 117.80, 114.78, 110.70, 109.76, 44.47, 12.56. HR-ESI-MS: m/z calcd [C₂₃H₂₁NO₆S] for 440.1090, found [M+H]⁺ = 440.1158.

Synthesis of Compound FNE6

Compound **3HFNE** (310 mg, 1 mmol), 5-quinoline sulfonyl chloride (272 mg, 1.2 mmol), and TEA (200 mg, 2 mmol) were added to DMF (10 mL). The solution was stirred at 40 °C for 6 h. The mixture was extracted with ethyl acetate (30 mL × 3). The combined organic layer was dried over MgSO₄, which was filtered, and the filtrate was evaporated. The crude yellow oil was purified by column chromatography (ethyl acetate: petroleum ether = 1: 5, V: V) to give a yellow solid. Yield, 420 mg, 84 %; m.p: 198-203°C, ¹H NMR (400 MHz, CDCl₃) δ: 9.15 (d, J = 8.0 Hz, 1H), 8.96 (d, J = 4.0 Hz, 1H), 8.23 (d, J = 8.0 Hz, 1H), 8.11 (d, J = 8.0 Hz, 2H), 7.63 - 7.53 (m, 5H), 7.42 (d, J = 8.4 Hz, 1H), 7.31 (t, J = 8.0 Hz, 1H), 6.24 (d, J = 8.0 Hz, 2H), 3.27 (q, J = 8.0 Hz, 4H), 1.12 (d, J = 12.0 Hz, 6H).¹³C NMR (100 MHz, CDCl₃) δ : 172.01, 159.35, 155.04, 151.03, 149.71, 148.09, 136.28, 134.26, 133.66, 131.98, 130.24, 129.82, 127.29, 125.97, 124.99, 124.58, 123.75, 122.84, 117.78, 114.43, 110.16, 44.27, 12.54. HR-ESI-MS: m/z calcd [C₂₈H₂₄N₂O₅S] for 501.1406, found [M]⁺=501.1480.

Synthesis of Compound FNE7

Compound **3HFNE** (310 mg, 1 mmol), 2-thiophene sulfonyl chloride (219 mg, 1.2 mmol), and TEA (200 mg, 2mmol) were added to DMF (10mL). The solution was stirred at 40 °C for 6 h. The mixture was extracted with ethyl acetate (30 mL × 3). The combined organic layer was dried over MgSO₄, which was filtered, and the filtrate was evaporated. The compound was purified by column chromatography (ethyl acetate: petroleum ether = 1:5, V: V) to give a yellow solid. Yield, 360 mg, 79 %; m.p: 136-141°C, ¹H NMR (400 MHz, DMSO) δ: 8.03 - 7.98 (m, 2H), 7.80 (t, J = 4.0 Hz, 1H), 7.71 - 7.67 (m, 4H), 7.48 (t, J = 8.0 Hz, 1H), 7.03 (t, J = 4.0 Hz, 1H), 6.58 (d, 2H), 3.36 (m, 4H), 1.09 (t, J = 8.0 Hz, 6H).¹³C NMR (100 MHz, DMSO) δ: 171.33, 159.34, 154.90, 150.18, 136.66, 136.20, 136.01, 134.80, 131.33, 130.71, 128.24, 125.96, 125.51, 123.59, 118.74, 114.12, 111.02, 44.25, 12.90. HR-ESI-MS: m/z calcd [C₂₃H₂₁NO₅S₂] for 456.0861, found [M]⁺ = 456.0931.

3. Spectra and biological studies

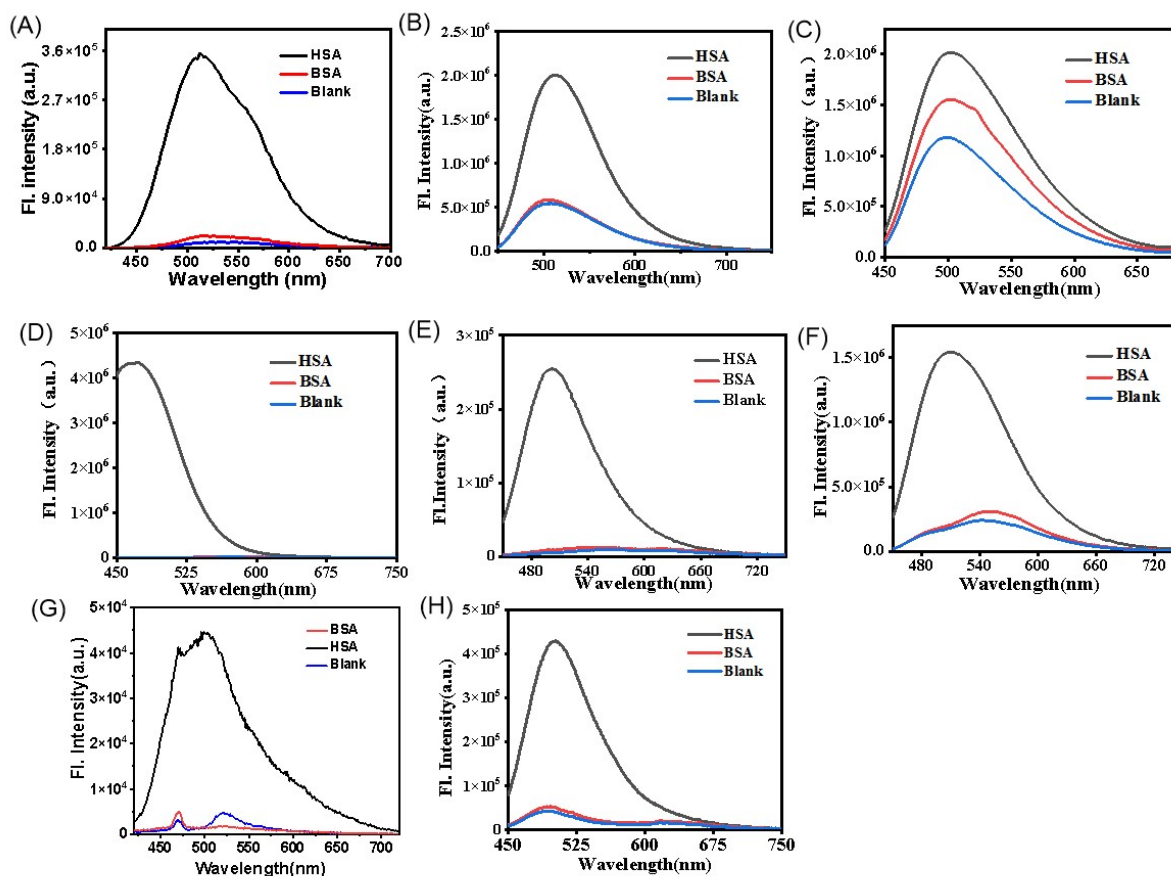


Figure. S1. The fluorescence spectra of 3HFNE (A), FNE1 (B), FNE2 (C), FNE3 (D), FNE4 (E), FNE5 (F), FNE6 (G) and FNE7 (H) in the presence of BSA and HSA. All probes and analytes are 5 μ M. All data were obtained after incubation in PBS buffer (0.01 M, pH 7.4) with the analytes at 37 $^{\circ}$ C. With excitation at 405 nm.

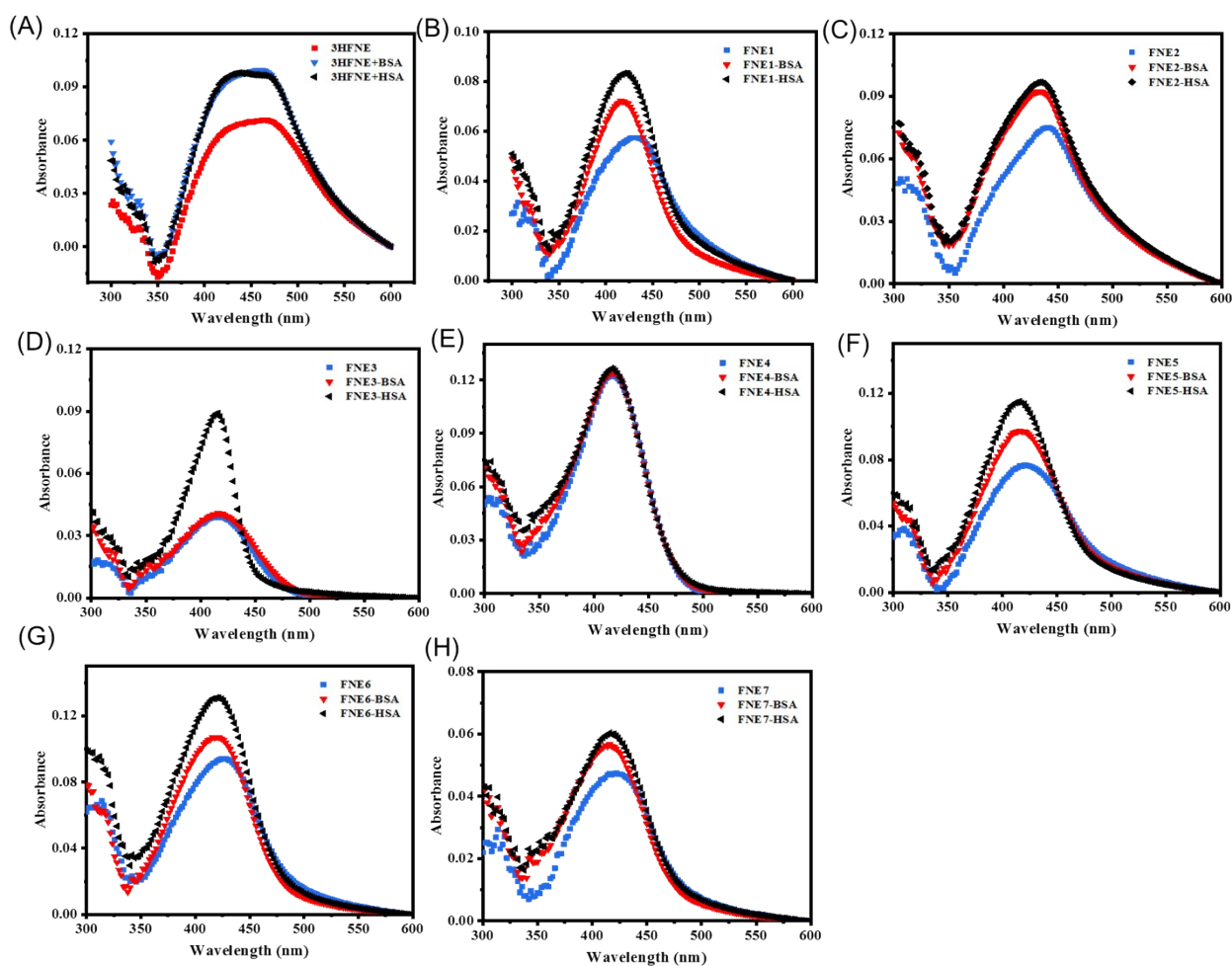


Figure. S2. The absorption spectra of 3HFNE (A), FNE1 (B), FNE2 (C), FNE3 (D), FNE4 (E), FNE5 (F), FNE6 (G) and FNE7 (H) in the presence of BSA and HSA. All probes and analytes are 5 μM . All data were obtained after incubation in PBS buffer (0.01 M, pH 7.4) with the analytes at 37 $^{\circ}\text{C}$.

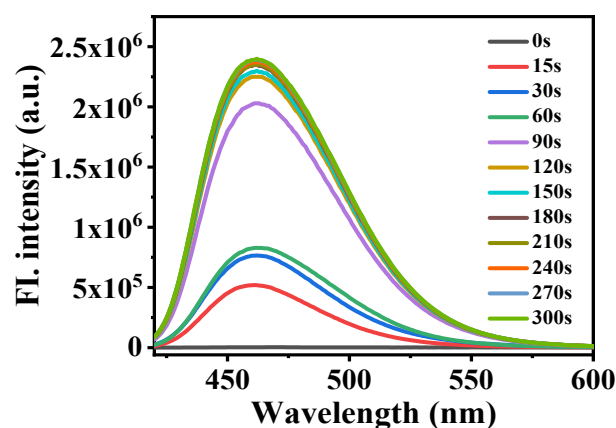
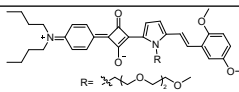
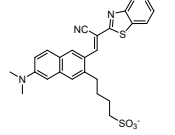
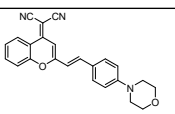
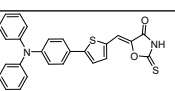
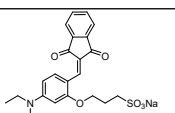
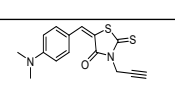
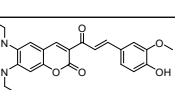
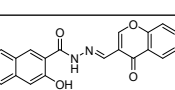
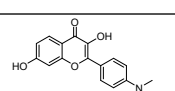
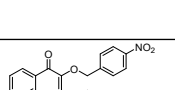
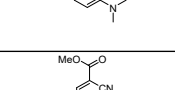
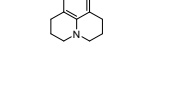


Figure. S3. Response time fluorescence spectra of 5 μM FNE3 and 5 μM HSA in PBS buffer (0.01 M, pH 7.4) at 37 $^{\circ}\text{C}$. λ_{ex} = 405 nm.

Table. S1. Comparison with representative fluorescent probes for HSA

Structure	Response model	Binding subdomain	LOD	Discriminate BSA	Response times(-fold) (HSA ranges)	Ref.
 <chem>R=C1=CC=C(C=C1)N(C)(C)C1=CC=C(C=C1)C(=O)O1C=CC=C(C=C1)O1</chem>	nucleophilic addition	Cys-34	3nM	No	/	<i>J. Am. Chem. Soc.</i> 2014 , 136, 13233-13239
 <chem>C1=CC=C2C=C(C=C1)C=C(C=C2)N(C)C1=CC=C(C=C1)S1=CC=C(N1)C#N</chem>	turn-on	IB	0.30 μg/mL	No	1000- 0-0.13 mg/mL	<i>ChemBioChem</i> 2019 , 20, 350-354
 <chem>C1=CC=C2C=C(C=C1)C=C(C=C2)N(C)C1=CC=C(C=C1)S1=CC=C(N1)C#N</chem>	turn-on	fatty acid site 1 (FA1)	0.25 μg/mL	Yes	60- 0-0.67 mg/mL	<i>Anal. Chim. Acta</i> 2021 , 1188, 339201
 <chem>C1=CC=C2C=C(C=C1)C=C(C=C2)N(C)C1=CC=C(C=C1)S1=CC=C(N1)C#N</chem>	turn-on	IB	0.34 μg/mL	No	60- 0-1 mg/mL	<i>ACS Biomater. Sci. Eng.</i> 2022 , 8, 253-260
 <chem>C1=CC=C2C=C(C=C1)C=C(C=C2)N(C)C1=CC=C(C=C1)S1=CC=C(N1)C#N</chem>	turn-on	/	0.253 μg/mL	Yes	450- 0-1 mg/mL	<i>Chem Asian J.</i> 2021 , 16, 1245-1252
 <chem>C1=CC=C2C=C(C=C1)C=C(C=C2)N(C)C1=CC=C(C=C1)S1=CC=C(N1)C#N</chem>	turn-on	IIA	0.3 μg/mL	Yes	700- 0-15 mg/mL	<i>Anal. Chim. Acta</i> 2018 , 1043, 123-131
 <chem>C1=CC=C2C=C(C=C1)C=C(C=C2)N(C)C1=CC=C(C=C1)S1=CC=C(N1)C#N</chem>	nucleophilic addition	lysine-161	/	Yes	16- 0-2 mg/mL	<i>Chem. Sci.</i> 2022 , 13, 218-224
 <chem>C1=CC=C2C=C(C=C1)C=C(C=C2)N(C)C1=CC=C(C=C1)S1=CC=C(N1)C#N</chem>	turn-on	IIA	0.70 μg/mL	/	141- 0-0.30 μg/mL	<i>J. Photoch. Photobio. A</i> 2022 , 422, 113576
 <chem>C1=CC=C2C=C(C=C1)C=C(C=C2)N(C)C1=CC=C(C=C1)S1=CC=C(N1)C#N</chem>	dual-emissive (495 / 575 nm)	IIIA	26 / 21 nM	No	/	<i>Chem. Commun.</i> 2020 , 56, 11094
 <chem>C1=CC=C2C=C(C=C1)C=C(C=C2)N(C)C1=CC=C(C=C1)S1=CC=C(N1)C#N</chem>	turn-on	IIA	32 nM	/	>60- 10 μM	<i>Chem. Commun.</i> 2019 , 55, 13983
 <chem>C1=CC=C2C=C(C=C1)C=C(C=C2)N(C)C1=CC=C(C=C1)S1=CC=C(N1)C#N</chem>	turn-on	IIA	0.4 μg/mL	Yes	400- 12.5 mM	<i>Chem. Commun.</i> 2014 , 50, 11507
 <chem>C1=CC=C2C=C(C=C1)C=C(C=C2)N(C)C1=CC=C(C=C1)S1=CC=C(N1)C#N</chem>	turn-on	IB	4.14 nM	Yes	1042- 0-5 μM	This work

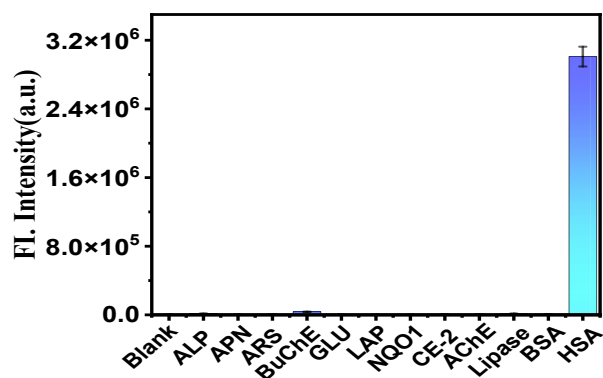


Figure. S4. The fluorescent intensity changes (at 463 nm) of 5 μM **FNE3** were obtained in the presence of various interfering analytes in PBS buffer (0.01 M, pH 7.4) at 37°C. Datas shown are for HSA (5 μM) and ALP (2 U/L), APN (100 ng/mL), ARS (1 U/mL), BChE (4 U/mL), GLU (100 $\mu\text{g/mL}$), LAP (50 U/L), NQO1 (500 ng/mL), CEL (10 $\mu\text{g/mL}$), AChE (4 U/mL) and Lipase (1 U/mL), respectively. $\lambda_{\text{ex}} = 405$ nm.

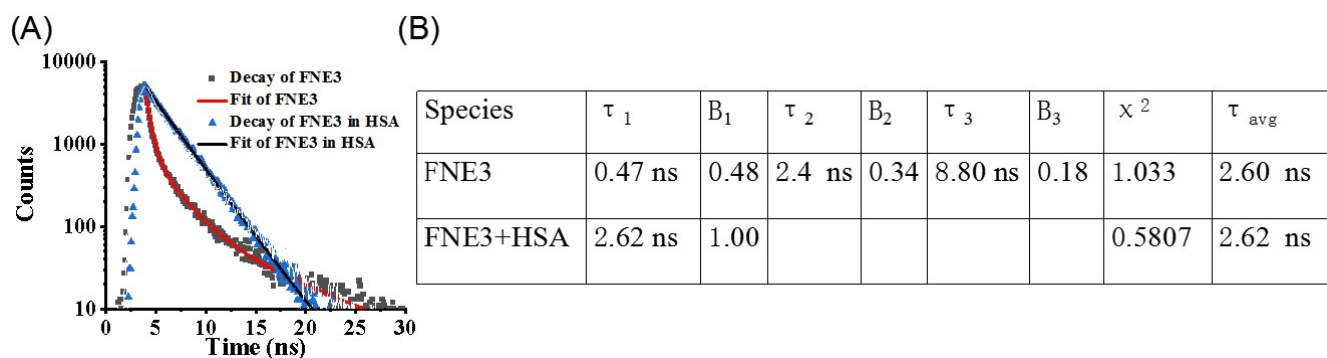


Figure. S5. (A) Fluorescence lifetime decay profiles ($\lambda_{\text{ex}} = 375$ nm) of free **FNE3** and **FNE3** with addition of HSA in PBS solution (0.01 M, pH 7.4). Red line represents FNE3, while blue line represents **FNE3**-HSA complex. (B) Time-resolved fluorescence decay parameters of **FNE3** with addition of HSA.

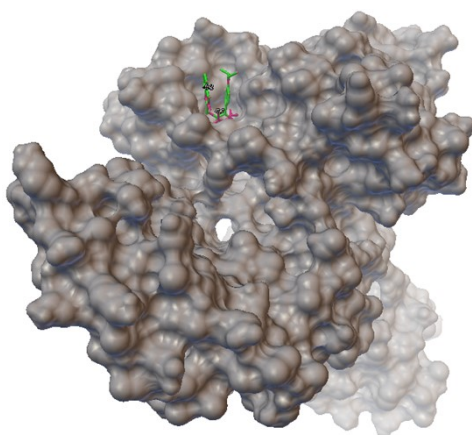


Figure. S6. The overview of **FNE3** (Green) and **DIF** (purple) bound into the subdomain IB of HSA. The surface of HSA was colored in gray.

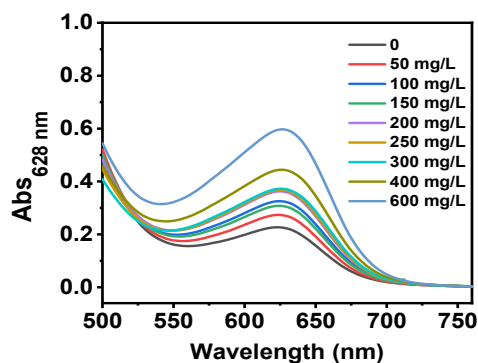


Figure. S7. Absorption spectra of **BCG** in the presence of different concentrations of HSA (0, 50, 100, 150, 200, 250, 300, 400, 600 mg/L) in PBS-diluted urines at 37°C.

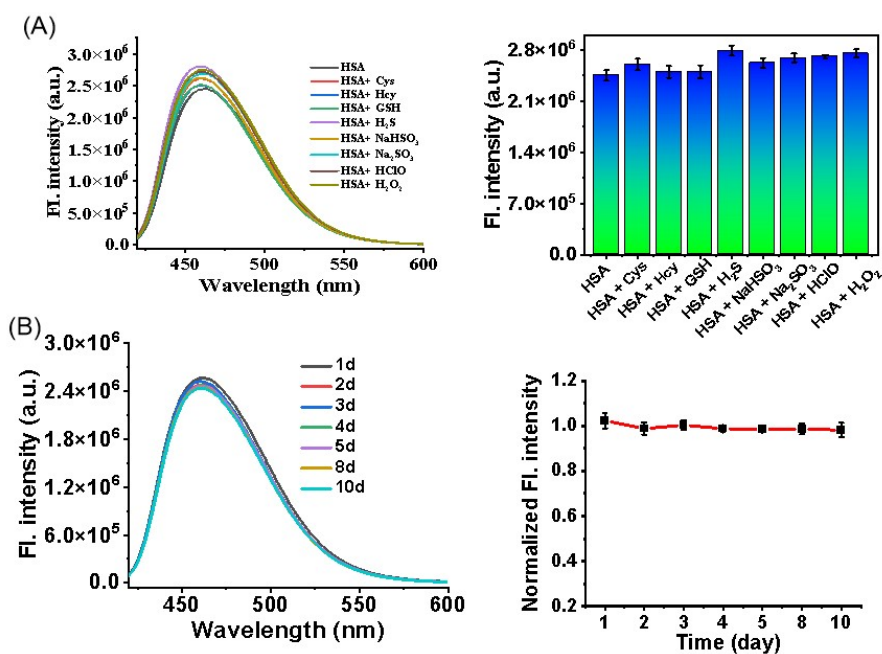


Figure. S8. (A) The chemical stability of 5 μM FNE3-HSA complex platform in the absence and presence of different nucleophiles, oxidants, and biological species including 200 μM Cys, 200 μM Hcy, 5 mM GSH, 200 μM H_2S , 200 μM NaHSO_3 , 200 μM Na_2SO_3 , 50 μM HClO , 100 μM H_2O_2 . $\lambda_{\text{ex}} = 405 \text{ nm}$. $\lambda_{\text{em}} = 463 \text{ nm}$. (B) Fluorescence spectra and intensity (at 463 nm) of 5 μM FNE3-HSA complex sensor in PBS solution at different times. $\lambda_{\text{ex}} = 405 \text{ nm}$. All test conditions were in PBS buffer (0.01 M, pH 7.4) at 37°C.

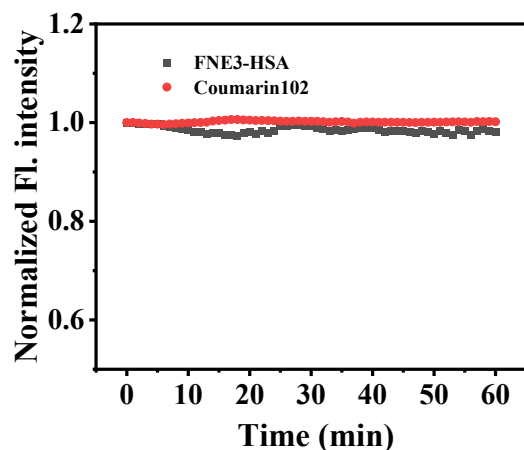


Figure. S9. Normalized time-dependent emission profile of **FNE3-HSA** fluorescent complex (5 μ M) and Coumarin 102 with continuous irradiation for 1 h in PBS (pH 7.4, 1% MeCN) at 37 $^{\circ}$ C using a Xe-lamp at 405 nm.

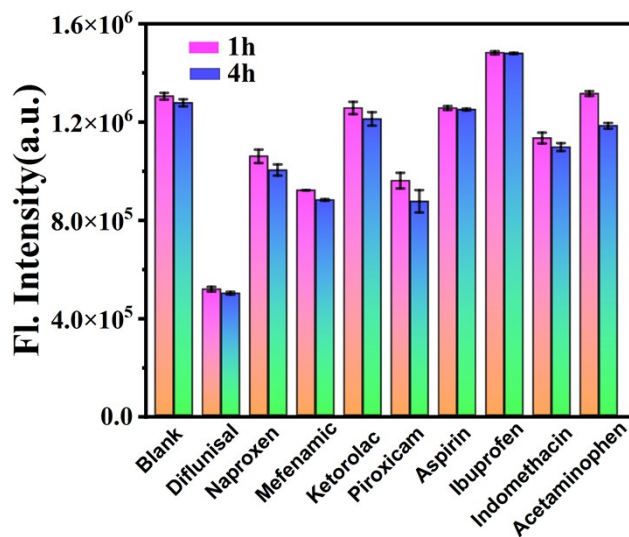
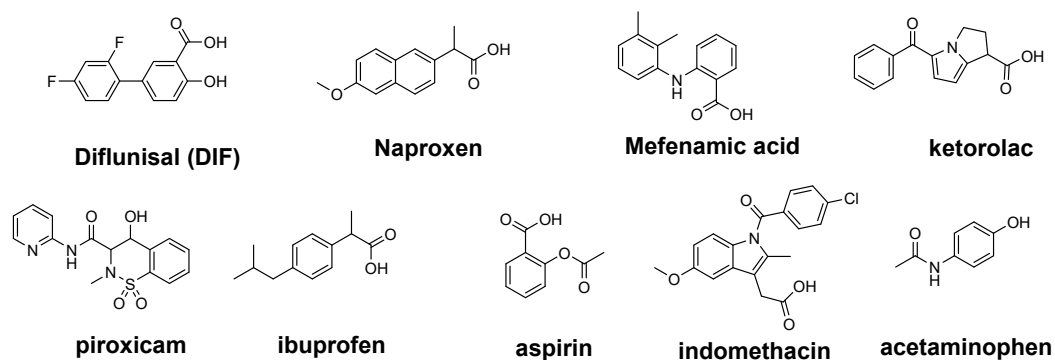


Figure. S10. The chemical structure of common clinical non-steroidal anti-inflammatory drugs in this study, such as diflunisal, naproxen, mefenamic, ketorolac, piroxicam, aspirin, ibuprofen, indomethacin, and acetaminophen. The selectivity of **FNE3-HSA** complex (5 μ M) for these common clinical non-steroidal anti-inflammatory drugs (50 μ M) for 1h or 4h in PBS (pH 7.4).

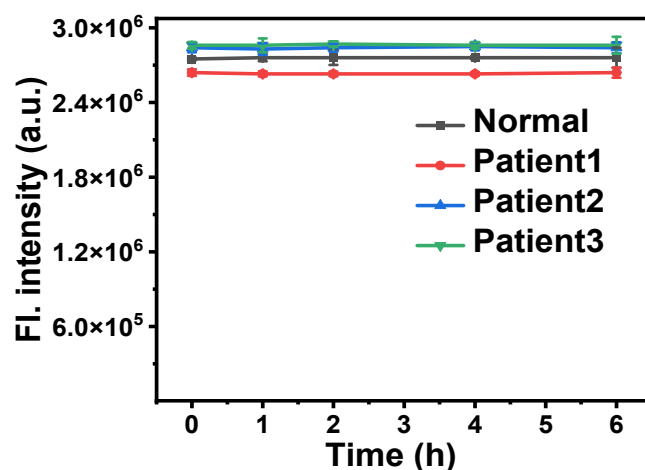


Figure. S11. The stability of FNE3-HSA complex (5 μM) in patient urine samples.

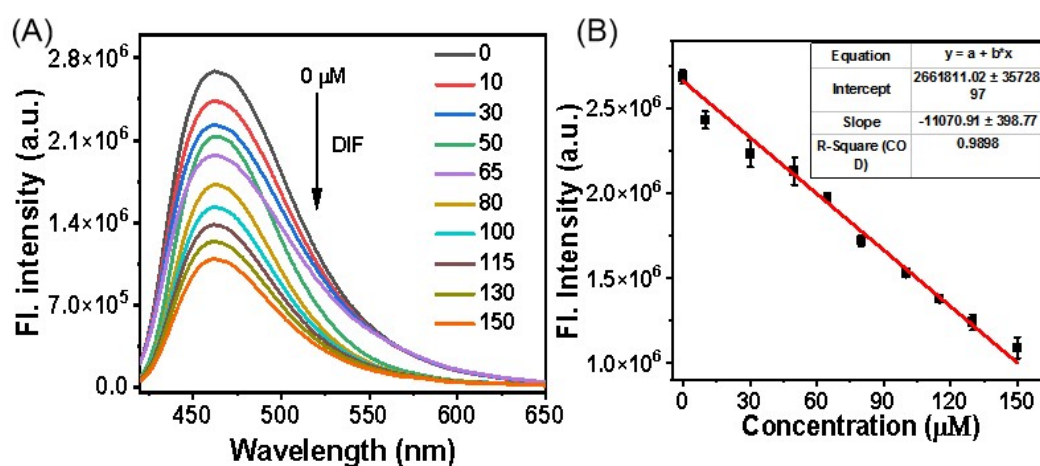


Figure. S12. (A) Fluorescent spectra of FNE3-HSA complex (5 μM) in the presence of different concentrations of DIF (0, 10, 30, 50, 75, 100, 150 μM) in PBS-diluted urine samples. (B) Linear response of fluorescence intensity at 463 nm for FNE3-HSA complex along with different DIF concentrations in urine samples.

Table S2. Recovery study of spiked DIF in diluted patient urine with FNE3-HSA fluorescent complex

Number	[DIF] added artificially (μM)	[DIF] detected by FNE3-HSA sensor (μM)	Recovery (n=3, %)
1	48.0	46.17 \pm 0.17	96.77
2	95.0	98.20 \pm 0.42	103.19
3	135.0	136.44 \pm 0.40	101.93

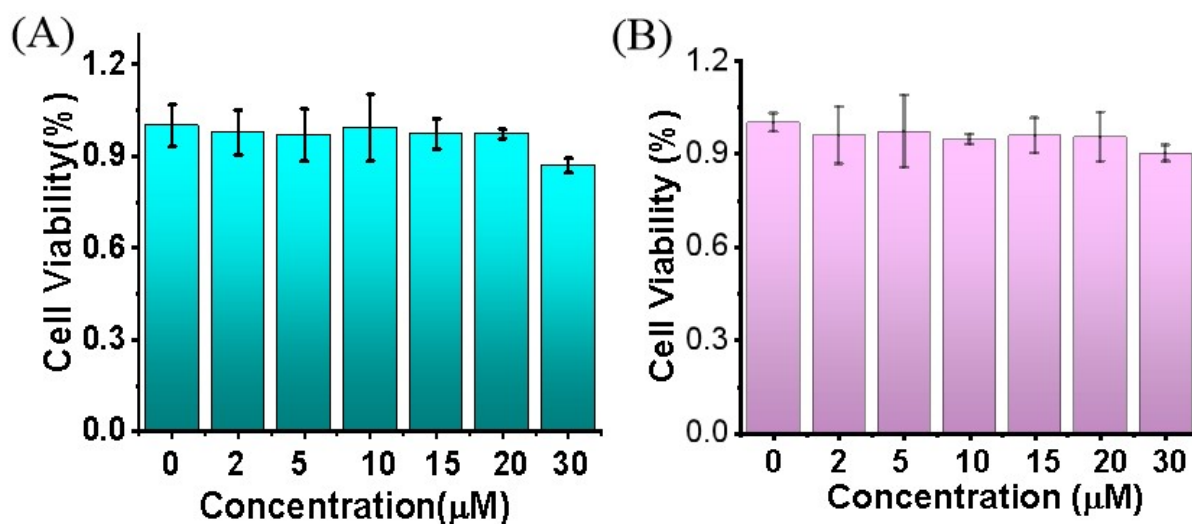


Figure. S13. Cell viabilities of HeLa cells treated with different concentrations (0-30 μM) of FNE3 and FNE3-HSA complex for 24 h.

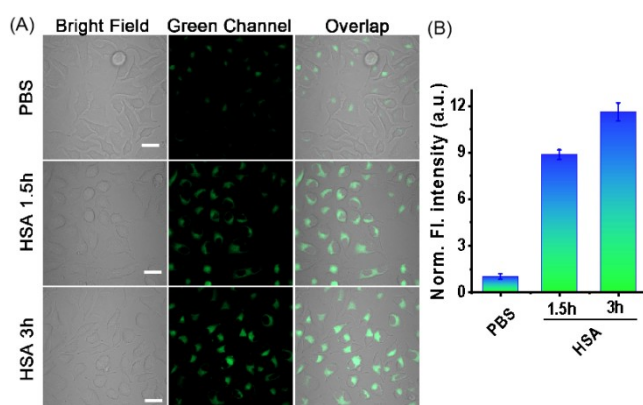


Figure. S14 (A) Confocal fluorescence images of FNE3 in HeLa cells. HeLa cells incubated with FNE3 (5 μM) for 1h, Images of HeLa cells after treatment with 25 μM HSA for 1.5h or 3h and subsequent treatment of the cells with FNE3 (5 μM) for 1h ($\lambda_{\text{ex}} = 405 \text{ nm}$, $\lambda_{\text{em}} = 425\text{--}475 \text{ nm}$); Scale bar: 20 μm . (B) Relative fluorescence intensity of red channel in cells were acquired from (A). Data represent mean standard error (n=3 independent experiments).

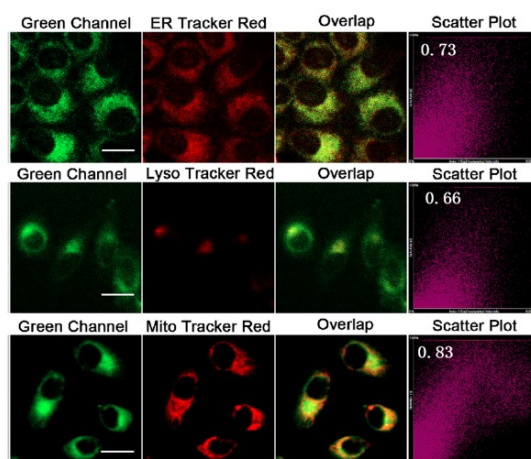
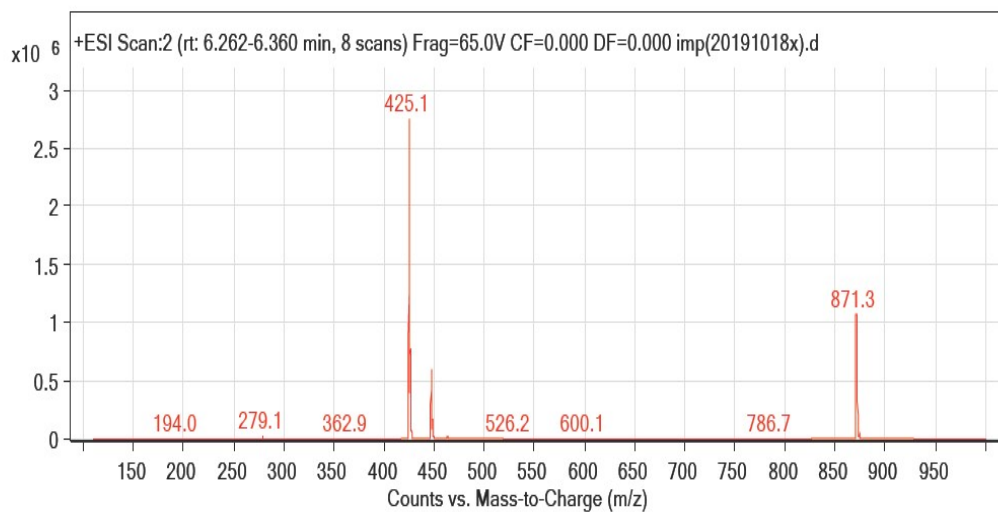
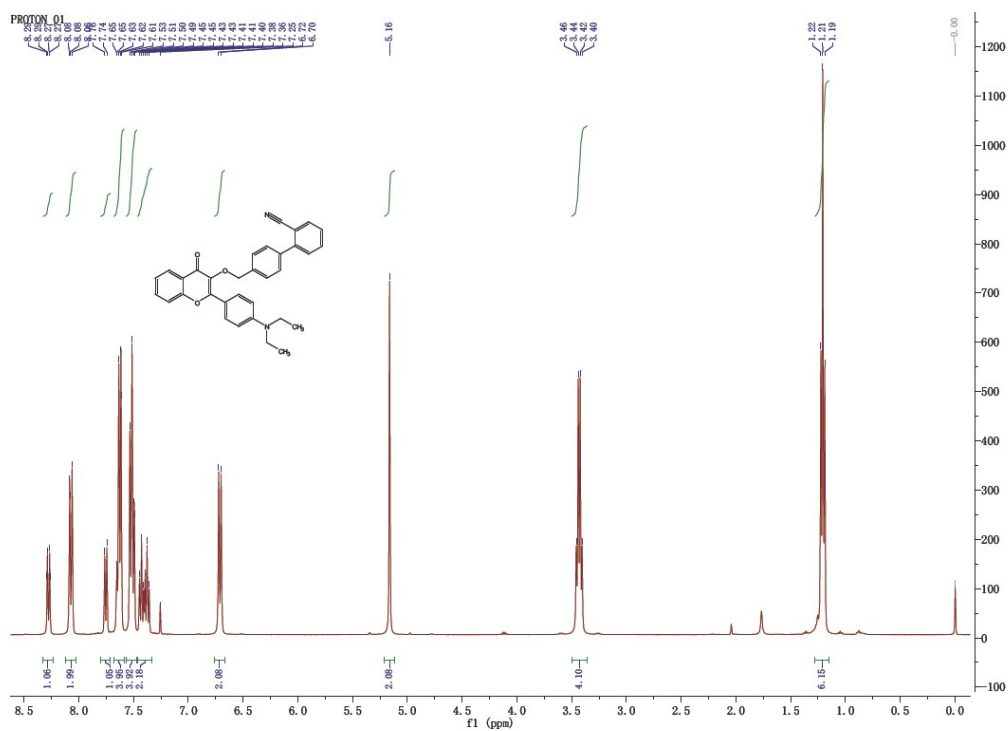


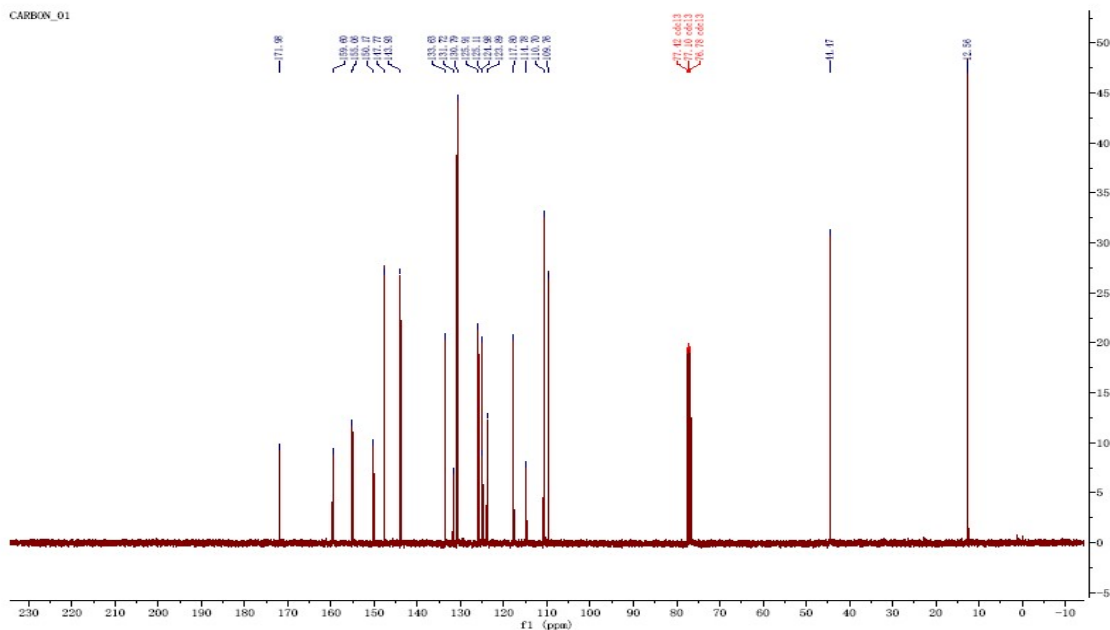
Figure. S15. Intracellular localization of FNE3-HSA complex in HeLa cells. Images of HeLa cells pretreated respectively with FNE3-HSA complex (5 μM) for 20 min and subsequently 0.2 μM Mito-Tracker Red or Lyso-Tracker Red or ER-Tracker Red for 10 min. Green channel, FNE3-HSA complex fluorescence ($\lambda_{\text{ex}} = 405 \text{ nm}$, $\lambda_{\text{em}} = 425\text{--}475 \text{ nm}$); red channel, Mito-Tracker Red, ER-Tracker Red and Lyso-Tracker Red fluorescence ($\lambda_{\text{ex}} = 560 \text{ nm}$, $\lambda_{\text{em}} = 580\text{--}675 \text{ nm}$); The overlapping images and colocalization of FNE3-HSA complex and Trackers, respectively. Scale bar: 20 μm .



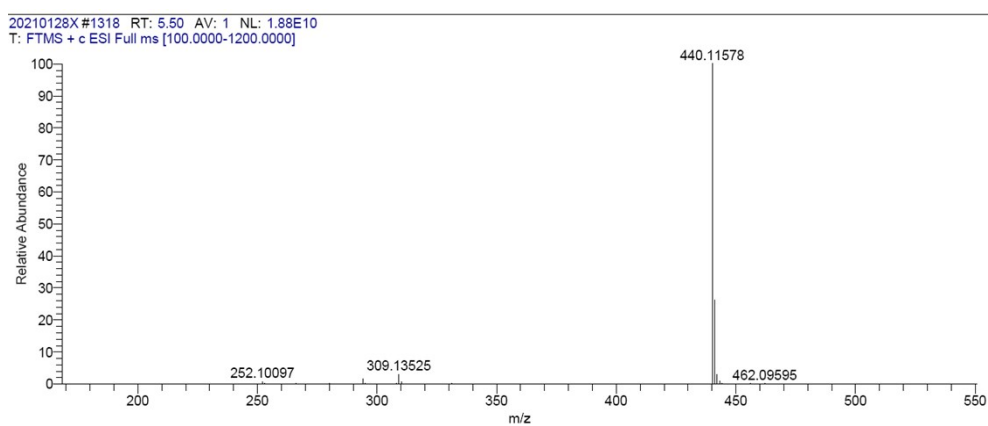
MS spectrum of compound **FNE1**



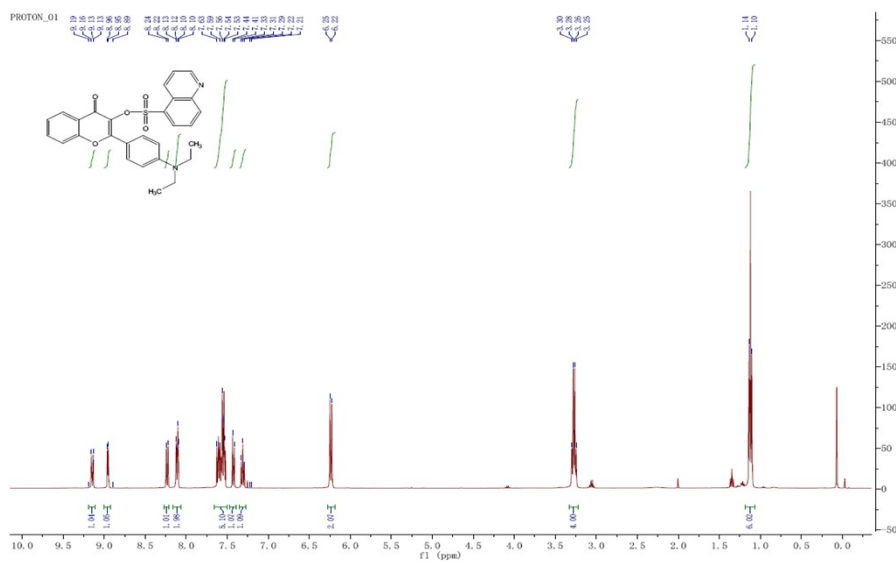
¹H NMR (400 MHz, CDCl₃) spectrum of compound **FNE2**



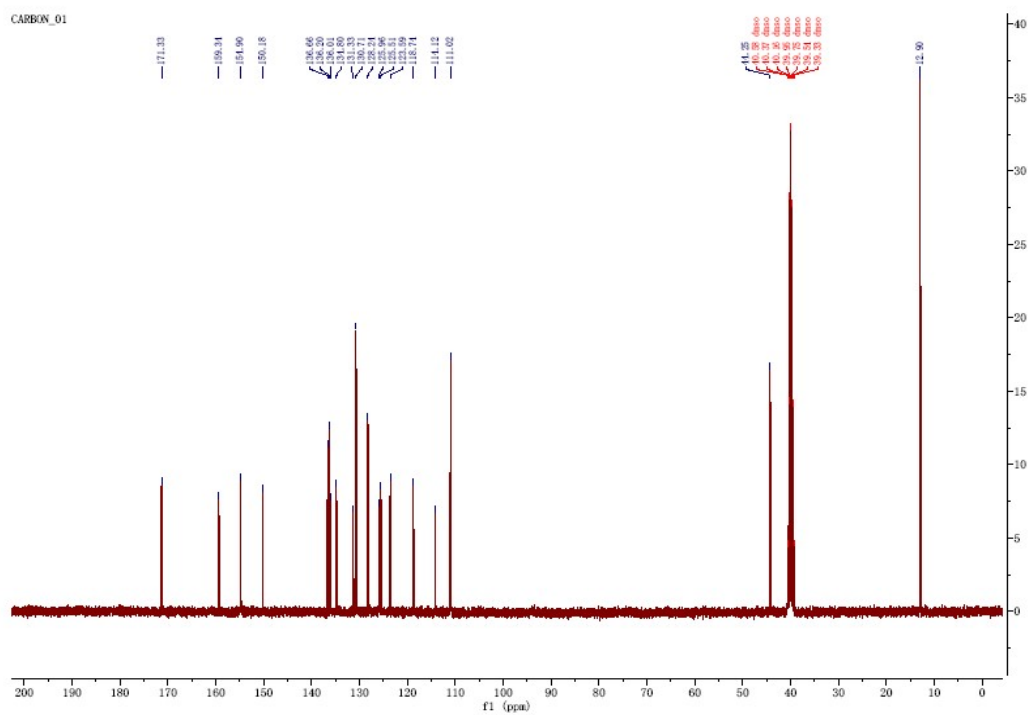
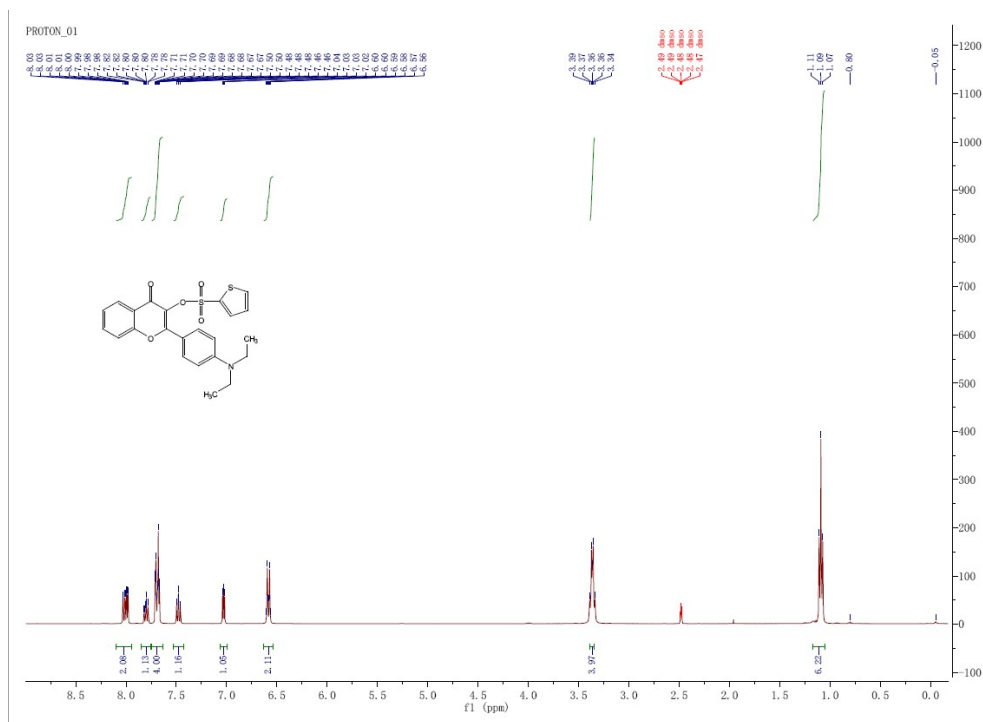
¹³C NMR (400 MHz, CDCl₃) spectrum of compound **FNE5**

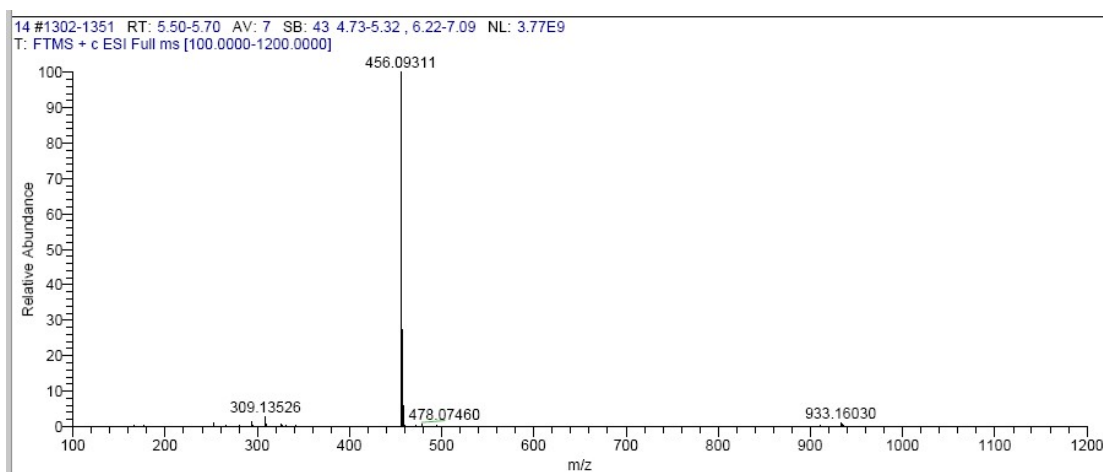


HRMS spectrum of compound **FNE5**



¹H NMR (400 MHz, CDCl₃) spectrum of compound **FNE6**





HRMS spectrum of compound **FNE7**

5. Supplemental References

- [1] O. Trott, A.J. Olson, AutoDock Vina: improving the speed and accuracy of docking with a new scoring function, efficient optimization, and multithreading, *J. Comput. Chem.*, 2010, **31**, 455-461.
- [2] A. N. Fletcher and D. E. Bliss, Laser dye stability. Part 5, *Appl. phys.*, 1978, **16**, 289-295.
- [3] M. Tian, J. Sun, Y. Tang, B. Dong, W. Lin, Discriminating Live and Dead Cells in Dual-Color Mode with a Two-Photon Fluorescent Probe Based on ESIPT Mechanism, *Anal. Chem.*, 2018, **90**, 998-1005.